Critical line in random-threshold networks with inhomogeneous thresholds

Thimo Rohlf
Max-Planck-Institute for Mathematics in the Sciences, Inselstraße 22, D-04103 Leipzig, Germany
(Received 21 February 2008; revised manuscript received 4 November 2008; published 30 December 2008)

We calculate analytically the critical connectivity K_c of random-threshold networks (RTNs) for homogeneous and inhomogeneous thresholds, and confirm the results by numerical simulations. We find a superlinear increase of K_c with the (average) absolute threshold $|h|$, which approaches $K_c(|h|) \sim h^2/(2\ln|h|)$ for large $|h|$, and show that this asymptotic scaling is universal for RTNs with Poissonian distributed connectivity and threshold distributions with a variance that grows slower than h^2. Interestingly, we find that inhomogeneous distribution of thresholds leads to increased propagation of perturbations for sparsely connected networks, while for densely connected networks damage is reduced; the crossover point yields a characteristic connectivity K_d, that has no counterpart in Boolean networks with transition functions not restricted to threshold-dependent switching. Last, local correlations between node thresholds and in-degree are introduced. Here, numerical simulations show that even weak (anti)correlations can lead to a transition from ordered to chaotic dynamics, and vice versa.

DOI: 10.1103/PhysRevE.78.066118 PACS number(s): 89.75.Da, 05.45.−a, 05.65.+b

I. INTRODUCTION

Many systems in nature, technology, and society can be described as complex networks with some flow of matter, energy, or information between the entities the system is composed of; examples are neural networks, gene regulatory networks, food webs, power grids, and friendship networks. Often, in particular when the networks considered are very large, many details of the topological structure as well as of the dynamical interactions between units are unknown, hence statistical methods have to be applied to gain insight into the global properties of these systems. In this spirit, Kauffman [1,2] introduced the notion of random-Boolean networks (RBNs), originally as a simplified model of gene regulatory networks (GRNs). In a RBN of size N, each node i receives inputs from $0 \leqslant k \leqslant N$ other nodes (with k usually either considered to be constant, or distributed according to a Poissonian with average $\bar{K} \ll N$), and updates its state according to a Boolean function f_i of its inputs; the subscript i indicates that Boolean functions vary from site to site, usually assigned at random to each node. It was shown that RBNs exhibit a percolation transition from ordered to chaotic dynamics at a critical connectivity $\bar{K}=K_c=2$.

In the theory of equilibrium critical phenomena often mean-field theories are applied as a first approach, neglecting possible higher-order correlations in the system. This idea also has been successfully applied to RBNs for analytical calculation of critical points, for example using the so-called *annealed approximation* introduced by Derrida and Pomeau [3–5]. The basic premise of the annealed approximation is that it neglects correlations between nodes and treats the system as if links were rewired randomly at each time step. This approximation has been applied for a variety of calculations, but it has proven to work most successfully for the analytical calculation of the propagation of perturbations (damage) [6]. Recent research has revealed many surprising details of RBN dynamics at criticality, e.g., superpolynomial scaling of the number of different dynamical attractors (fixed points or periodic cycles) with N [7] (while Kauffman assumed it to scale $\sim\sqrt{N}$ [1]), as well as analytically derived scaling laws for mean attractor periods [8] and for the number of frozen and relevant nodes in RBNs [9,10]. Similarly, it was shown recently that dynamics in finite RBNs exhibits considerable deviations from the annealed approximation (that is, exact only in the limit $N \to \infty$) [11,12]. Boolean network models have been applied successfully to model the dynamics of real biological systems, e.g., the segment polarity network of *Drosophila* [13], dynamics and robustness of the yeast cell cycle network [14], damage spreading in knock-out experiments [15], as well as establishment of position information [16] and cell differentiation [17] in development. Other models explicitly evolve RBN topology according to local rewiring rules coupled to local order parameters of network dynamics (e.g., the local rate of state changes), and investigate the resulting self-organized critical state [18–20].

A drawback of RBNs is the fact that, in spite of their discrete nature (which makes them easy to simulate on the computer in principle), the time needed to compute their dynamics in many instances scales exponentially in N and $\bar{K}$, and often large statistical ensembles are needed for unbiased statistics due to the strongly nonergodic character [21] of RBN dynamics. For this reason, there exists considerable interest in simplified models of RBN dynamics, as, for example, *random-threshold networks* (RTNs), that constitute a subset of RBNs.

In RTNs, states of network nodes are updated according to a weighted sum of their inputs plus a threshold h, while interaction weights take (often discrete and binary) positive or negative values assigned at random. The critical connectivity, calculated by means of the annealed approximation, was found to deviate slightly from RBNs [22–24]; this analysis was extended to RTN dynamics including stochastic update errors [25]. In particular, it was found that phase transitions in RTNs with scale-free topologies [25,26] substantially differ from both RTNs with homogeneous or Poissonian distributed connectivity and scale-free RBNs [27]. Further, dynamics in finite RTNs with $k=\text{const}=2$ inputs per node recently was found to be surprisingly ordered, including, e.g.,

globally synchronized oscillations [28]. Other approaches, that apply learning algorithms as well as ensemble techniques, present evidence that information processing of static [29] or time-variant [30] external inputs is optimized at criticality in both RBNs and RTNs.

In this paper, we extend the theoretical analysis of RTNs in a number of respects. First, we calculate the critical connectivity K_c for arbitrary thresholds $h \leqslant 0$, and generalize this derivation to inhomogeneously distributed thresholds h_i that can vary from node to node. This generalization, that introduces an additional level of complexity to RTN dynamics, is motivated by recent observations of strong variations in regulatory dynamics from gene to gene in real GRNs, caused by, for example, the frequent occurrence of canalizing functions [21] and the abundance of regulatory RNA in multicellular organisms which strongly influence the expression levels and patterns of (regulatory) proteins [31–33]. Using the annealed approximation and additional approximation techniques, we derive a general scaling relationship between critical connectivity K_c and (average) absolute node threshold $|h|$, and show that $K_c(|h|)$ asymptotically approaches a unique scaling law $K_c(|h|) \sim h^2/(2 \ln|h|)$ for large $|h|$. Evidence is presented that this asymptotic scaling law is universal for RTNs with Poissonian distributed connectivity and threshold distributions with a variance that grows slower than $|h|^2$. Convergence against this scaling law is rather slow (logarithmic in $|h|$); we show that, for finite $|h|$, scaling behavior can be approximated well locally by power laws $K_c(|h|) \sim |h|^\alpha$ with $3/2 < \alpha < 2$.

Further, we establish that damage propagation functions of RTNs with homogeneous thresholds $|h|$ and of RTNs with inhomogeneous thresholds with the same *average* $|\bar{h}| = |h|$ intersect at characteristic connectivities $K_d(|h|) > K_c(|h|)$, which implies that for $\bar{K} < K_d$, random distribution of thresholds tends to increase damage, while for $\bar{K} > K_d$, the opposite holds. Evidence is presented that $K_d(|h|)$ converges to an asymptotic scaling law $K_d(|h|) \sim h^2$. We compare the scaling of K_d to the corresponding case of random-Boolean networks (RBNs) with inhomogeneously distributed bias, parametrized in terms of a bias parameter $1/2 \leqslant p \leqslant 1$. It is shown that K_d *is not defined for RBNs* in the limit $p \to 1$, which corresponds to $|h| \to \infty$ in RTNs. Hence K_d constitutes an interesting concept, yielding a different characteristic connectivity which is well-defined only for RTNs.

Last, we investigate the effect of correlations between thresholds h_i and in-degree k_i, while keeping all other network parameters constant. We find that even small positive correlations can induce a transition from supercritical (chaotic) to subcritical (ordered) dynamics, while anticorrelations have the opposite effect. These observations also hold for large initial perturbations, and positive correlations are shown to have the same effect as a decrease in the average wiring density of networks by several percent. Further, positive correlations significantly reduce the variance of the damage, and hence may lead to a supression and better control of extreme damage events.

The results of our study are summarized in Sec. IV and possible implications for RTN-based models of gene regulatory networks [34–36] are discussed.

II. RANDOM-THRESHOLD NETWORKS

A random-threshold network (RTN) consists of N randomly interconnected binary sites (spins) with states $\sigma_i = \pm 1$. For each site i, its state at time $t+1$ is a function of the inputs it receives from other spins at time t:

$$\sigma_i(t+1) = \mathrm{sgn}[f_i(t)] \tag{1}$$

with

$$f_i(t) = \sum_{j=1}^{N} c_{ij}\sigma_j(t) + h_i, \tag{2}$$

where c_{ij} are the interaction weights. If i does not receive signals from j, one has $c_{ij}=0$, otherwise, interaction weights take discrete values $c_{ij} = \pm 1, +1$, or -1 with equal probability. In the following discussion we assume that the threshold parameter takes integer values $h_i \leqslant 0$ [37]. Further, we define $\mathrm{sgn}(0) = -1$ [38]. The N network sites are updated *synchronously*. Notice that we depart from the well-studied case $h_i = \mathrm{const} = 0$ in two respects: h_i can take arbitrary values $h_i \leqslant 0$, and it can differ from node to node (inhomogeneous thresholds).

Let us now have a closer look on network topology. Let $\bar{K}$ be the *average connectivity*, i.e., the average number of inputs (outputs) per site, and let us assume that each interaction weight has equal probability $p = \bar{K}/N$ to take a nonzero value. Further, let us consider the limit of sparsely connected networks with $\bar{K} \ll N$. Under these assumptions, the statistical distribution ρ_k of in- and out-degrees follows a Poissonian:

$$\rho_k = \frac{\bar{K}^k}{k!} e^{-\bar{K}}. \tag{3}$$

Concerning thresholds h_i, we will consider four cases: constant, negative thresholds $h_i = \mathrm{const} \leqslant 0$, thresholds distributed according to a Poissonian around the average (absolute) threshold $|\bar{h}|$, thresholds distributed according to a discretized Gaussian, and Poissonian distributed thresholds that are correlated to k.

III. CALCULATING THE CRITICAL LINE

A. Uniform threshold $h < 0$

We start with the simplest case and assume that all network sites have identical integer threshold values $h_i \equiv h \leqslant 0$. The case $h > 0$ is not studied here, as it may lead to the pathological outcome of nodes set to an active state $\sigma_i = +1$, though they receive only inhibitory inputs $c_{ij} < 0$.

Let us first calculate the probability for damage spreading $p_s(k)$, i.e., the probability that a node with k inputs changes its state, if one of its input states is flipped. A straightforward extension of the combinatorial analysis carried out in [24] for the special case $h=0$ yields

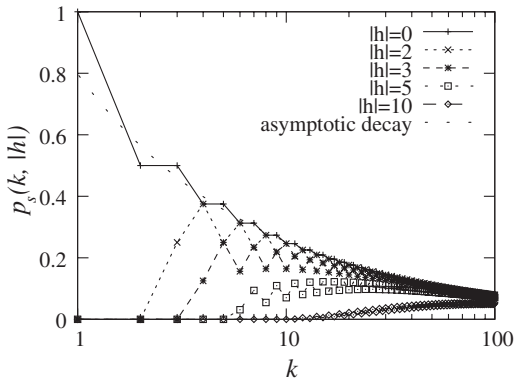

FIG. 1. Probability $p_s(k,|h|)$ of damage propagation, for different values of the threshold $|h|$, as a function of the number of inputs k. For large k, the curves asymptotically approach $p_s \sim 1/\sqrt{k}$ (dashed line). Notice the oscillatory behavior for $|h|>0$.

$$p_s(k,|h|) = k^{-1}2^{-(k+1)}\left[(k+|h|+1)\binom{k}{\frac{k+|h|+1}{2}} + (k-|h|+1)\binom{k}{\frac{k-|h|+1}{2}}\right] \tag{4}$$

$$= 2^{-(k-1)}\binom{k-1}{\frac{k+|h|-1}{2}} \tag{5}$$

for odd $k-|h|$ with $k>|h|$, and

$$p_s(k,|h|) = k^{-1}2^{-(k+1)}\left[(k-|h|)\binom{k}{\frac{k-|h|}{2}} + (k+|h|+2)\binom{k}{\frac{k+|h|+2}{2}}\right] \tag{6}$$

$$= 2^{-(k-1)}\binom{k-1}{\frac{k+|h|}{2}} \tag{7}$$

for even $k-|h|$ with $k>|h|$ (for a detailed derivation, please refer to Appendix A). Notice that Eqs. (5) and (7) are similar, yet not identical to the corresponding relations derived in [25] for RTNs with probabilistic time evolution; in particular, for the RTN with *deterministic* dynamics as studied here, the relation $p_s^{\text{odd}}(k)=p_s(k-1)$ holds only for the special case $|h|=0$, whereas for $|h|>0$, $p_s(k)$ exhibits an oscillatory behavior (Fig. 1).

If we know the statistical distribution function ρ_k of the in-degree, the average damage spreading probability $\langle p_s\rangle$ per link, where $\langle\cdot\rangle$ indicates the average over the ensemble of all possible network topologies that can be generated according to the degree distribution ρ_k, can be obtained by averaging over the nodes' individual damage spreading probabilities. To calculate this quantity, one has to divide the expected damage per node, $\bar{d}=\Sigma_{k=|h|}^{\infty} k\rho_k p_s(k,|h|)$, by the average number of links $\bar{K}$, which gives for the probability that a randomly picked link c_{ij} propagates damages from node j to node i:

$$\langle p_s\rangle(\bar{K},|h|) = \frac{1}{\bar{K}}\sum_{k=|h|}^{\infty} k\rho_k p_s(k,|h|). \tag{8}$$

In particular, in the case of a Poisson distributed connectivity with average degree $\bar{K}$, it follows that

$$\langle p_s\rangle(\bar{K},|h|) = e^{-\bar{K}}\sum_{k=|h|}^{N}\frac{\bar{K}^k}{k!}p_s(k+1,|h|). \tag{9}$$

A derivation of this relation, together with a discussion of its range of applicability, is provided in Appendix B [39]. Let us now apply the *annealed approximation* [3], which averages the effect of perturbations over the whole ensemble of possible network topologies *and* all accessible state configurations. Starting from a random initial state, the set of input state configurations contributing to damage propagation covers all possible configurations. For the evaluation of the critical point, however, it is essential to consider the propagation of a perturbation in the stationary state, and in this case more care has to be applied. In the stationary state, one has to average over all input states that have the *correct proportion* of +1 and −1 states. For the networks considered in our study, this set is identical with the full (binomial distributed) set of input states, since half of the connections are inhibitory, which means that a node sees inputs half of which are +1 and half of which are −1 (on average). Hence we can approximate the expected damage $\bar{d}$ after one update time step, given that a one-bit perturbation at time $t-1$ is by

$$\bar{d}(t+1) = \langle p_s\rangle(\bar{K},|h|)\bar{K}, \tag{10}$$

where $\bar{\cdot}$ denotes the average over all possible network topologies and all possible state configurations. If we apply a sufficiently large (but finite) upper limit N to the sum in Eq. (9), we can numerically evaluate this formula with any desired accuracy. Figure 2 shows the results for the first five values of negative h of RTNs with Poissonian distributed connectivity, compared to measurements obtained from numerical simulations of large ensembles of randomly generated instances of RTNs, indicating an excellent match between theory and simulation.

B. Poisson distributed thresholds

Let us now consider the more general case of nonuniform thresholds, i.e., networks where each site i has assigned an individual threshold $h_i \leqslant 0$. In the simplest case, we can imagine that the final thresholds resulted from iterated, random decrementations (starting from $h=0$ for all sites), until a certain average threshold $\bar{h}$ is reached—this process results in Poisson distributed thresholds h_i. If threshold assignment is independent from the (also Poisson distributed) in-degree,

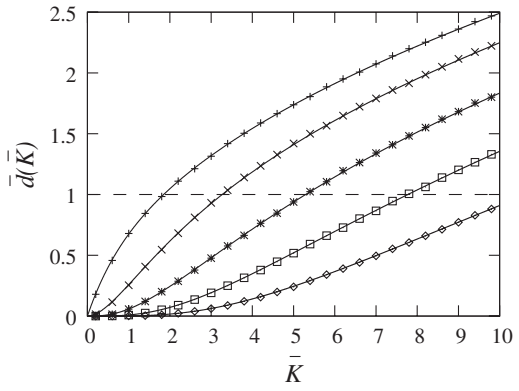

FIG. 2. Expectation value $\bar{d}$ of damage one time step after a one-bit perturbation, as a function of the average connectivity $\bar{K}$, and different (homogeneous) thresholds $|h|$ [$|h|=0$ (+), $|h|=1$ (×), $|h|=2$ (*), $|h|=3$ (□), $|h|=4$ (◇)]. Solid curves are the corresponding analytical results obtained from the annealed approximation.

the probabilities for k and h simply multiply, and the resulting average damage propagation probability is

$$\langle p_s\rangle(\bar{K},|\bar{h}|) = e^{-(\bar{K}+|\bar{h}|)} \sum_{|h|=0}^{N} \sum_{k=|h|}^{N} \frac{\bar{K}^k |\bar{h}|^{|h|}}{k!|h|!} p_s(k+1,|h|), \quad (11)$$

where $|\bar{h}|$ is the average absolute threshold.

Figure 3 demonstrates that the expected damage $\bar{d}_{t+1}(\bar{K},|\bar{h}|)$ resulting from a one-bit perturbation at time t, as predicted from this annealed approximation over both degree and threshold distribution, exhibits excellent agreement with the results obtained from numerical simulations of randomly generated RTN ensembles. It is an interesting question how the dynamics of RTNs with inhomogeneous thresholds compares to RTNs with homogeneous thresholds. Figure 4 shows

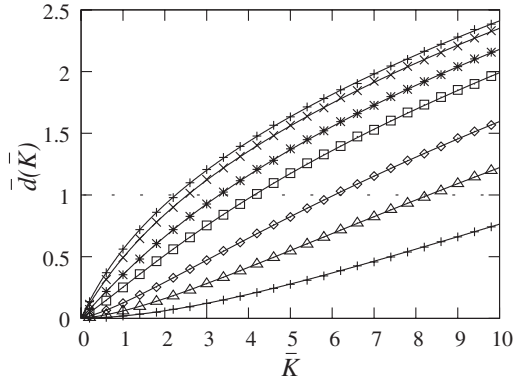

FIG. 3. Average damage $\bar{d}(\bar{K})$ one time step after a one-bit perturbation, for Poisson-distributed connectivity with average degree $\bar{K}$, and Poisson-distributed negative thresholds with average absolute value $|\bar{h}|$; points are data from numerical simulations of RTNs (ensemble averages over 100 000 different network realizations for each data point), lined curves are analytical solutions (annealed approximation). Numerical data were sampled for $|\bar{h}|=0$ (+), $|\bar{h}|=0.3$ (×), $|\bar{h}|=1.0$ (*), $|\bar{h}|=1.5$ (squares), $|\bar{h}|=2.5$ (◇), $|\bar{h}|=3.5$ (triangle), and $|\bar{h}|=5.0$ (+).

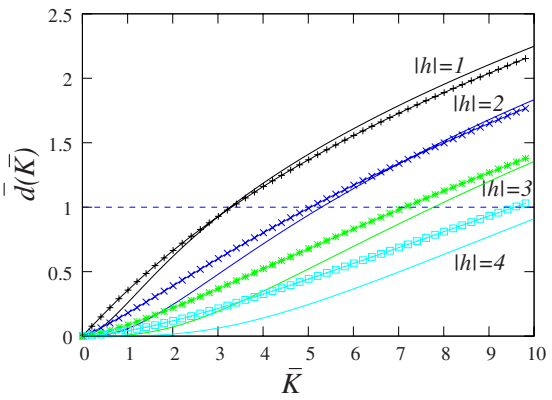

FIG. 4. (Color online) Comparison of damage spreading in networks with homogenenous thresholds $|h|=$const (solid lines, threshold values $|h|$ as indicated) vs networks with inhomogeneous thresholds distributed according to a Poissonian with the same *average* threshold $|\bar{h}|$ (curves with data points, $|\bar{h}|=1$ (+), $|\bar{h}|=2$ (×), $|\bar{h}|=3$ (*), and $|\bar{h}|=4$ (□); results obtained from the annealed approximation.

$\bar{d}(\bar{K})$ for RTNs with different homogeneous $|h|=$const. and the corresponding inhomogeneous RTNs with Poisson-distributed thresholds with the same *average* $|\bar{h}|=|h|$, as obtained from the annealed approximation. One observes that for small $\bar{K}$, the curves for RTNs with inhomogeneously distributed thresholds are systematically above those of the corresponding homogeneous RTNs, i.e., the randomization of node thresholds increases dynamical disorder—also, the critical connectivities $K_c(|h|)$ (intersections with the line $\bar{d}=1$) are shifted to smaller values. However, one also realizes that the curves intersect in the supercritical phase at characteristic connectivities $K_d(|h|)$, i.e., for $\bar{K}>K_d(|h|)$, inhomogeneity in thresholds actually *reduces* damage.

C. Universal scaling of the critical line

If we again assume a one-bit perturbation at time t, the critical line $K_c(|h|)$, that separates the ordered and the chaotic phase of RTN dynamics, is given by the condition

$$\bar{d}(t+1) = \langle p_s\rangle(K_c(|h|),|h|)K_c(|h|) = 1. \quad (12)$$

Again, we can apply Eq. (9) to solve this equation for arbitrary $h \leqslant 0$, however, numerical evaluation is almost impossible for $|h|>80$ due to exponentially diverging computing time caused by evaluation of the sum in Eq. (12) for large $\bar{K}$ [40]. For estimation of the scaling behavior of $K_c(|h|)$ for larger $|h|$, we are interested in a good approximation that does not require summation over the whole network topology, and hence neglect the variation in k, considering damage propagation in the *mean field limit* $k=\text{const}\approx\bar{K}$ (for details, see Appendix B). Using the Stirling approximation, $n!\approx n^n e^{-n}\sqrt{2\pi n}$, this leads to the following approximation for the logarithm of the damage:

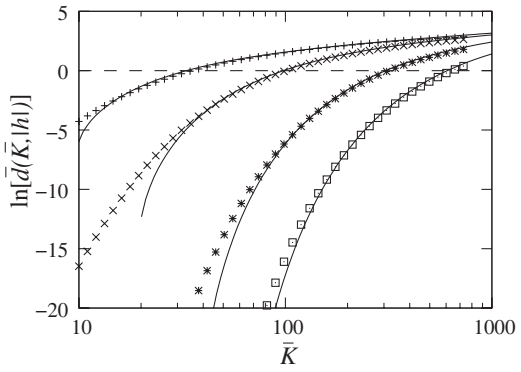

FIG. 5. Logarithm of the average damage, $\ln[\bar{d}(\bar{K})]$, as calculated from the annealed approximation, for different values of $|h|$ [$|h|=10$ (+), $|h|=20$ (×), $|h|=40$ (*), and $|h|=60$ (□)]. The corresponding solid curves are obtained from Eq. (13). For not too small $\bar{K}$, one finds that Eq. (13) approximates the true damage function very well.

$$\ln[\bar{d}(\bar{K},|h|)] \approx \frac{1}{2}\left\{ \ln \bar{K} - \bar{K} \ln\left[1 - \left(\frac{|h|}{\bar{K}}\right)^2\right] - |h| \ln\left[\frac{\bar{K}+|h|}{\bar{K}-|h|}\right]\right\} + C \tag{13}$$

with $C=\ln(\sqrt{2/\pi})$; solving this equation for

$$\ln[\bar{d}(K_c(|h|),|h|)] = 0 \tag{14}$$

then yields the critical connectivity $K_c(|h|)$. Figure 5 shows that this approximation is very accurate even for considerably small, finite $|h|$. In particular, one can show that for $|h| \geqslant 10$ the relative error ϵ between the approximation of Eq. (14) and the result obtained from the annealed approximation vanishes $\sim |h|^{-1}$ (Fig. 7).

Still, Eq. (14) has to be solved numerically to calculate $K_c(|h|)$, and hence does not yield information about the scaling behavior in the limit $|h| \to \infty$. A first insight into the expected scaling can be obtained from an analysis of the scaling behavior of the maximum of $p_s(k,|h|)$ with respect to $|h|$; if we restrict our analysis to even $k-|h|$, k_{max} is given by the condition

$$\Delta p_s = p_s(k,|h|) - p_s(k-2,|h|) \approx 0 \tag{15}$$

or, more accurately, we have to find the minimum of the absolute value $|\Delta p_s/\Delta k|$ of the "discrete derivative" of $p_s(k,|h|)$ for even $k-|h|$, with $\Delta k=\text{const}=2$. Inserting Eq. (7) then yields

$$\Delta p_s = 2^{-k+3} \frac{(k-3)!}{[(k+|h|-3)/2]![(k-|h|-3)/2]!} \times \left\{ \frac{(k-1)(k-2)}{(k+|h|+1)(k-|h|-1)} - 1 \right\}. \tag{16}$$

Obviously, the prefactor on the right-hand side is always positive; consequently, in order to determine the maximum of $p_s(k,|h|)$, we have to solve the equation

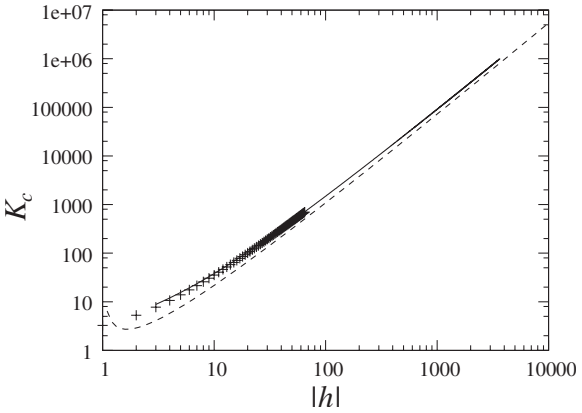

FIG. 6. Scaling behavior of the critical connectivity $K_c(|h|)$ as a function of the (homogeneous) node threshold $|h|$, log-log plot. Data points + are solutions obtained from the annealed approximation of Eq. (12), the solid curve is obtained from setting Eq. (13) to zero. The dashed line shows the asymptotic scaling behavior stated in Eq. (20).

$$\frac{(k-1)(k-2)}{(k+|h|+1)(k-|h|-1)} - 1 = 0. \tag{17}$$

Using simple algebra, one can show that

$$k_{\max} = |h|^2 + 1 \tag{18}$$

solves this equation, i.e., the maximum of $p_s(k,|h|)$ scales quadratically with $|h|$. Since $p_s(k,|h|)$ for $|h| \gg 0$ vanishes both for small and large k, it is plausible that the scaling behavior of K_c is dominated by the leading behavior of the maximum of the distribution, i.e., should scale $\sim f(|h|)|h|^2$, where contributions from the tails of the distribution are considered in $f(|h|)$.

A more detailed analysis carried out in Appendix D takes into account that, for large $\bar{K}$ and $|h|$, according to the central limit theorem the Binomial distribution that characterizes the damage propagation function Eq. (7) can be replaced by a Gaussian, consequently, the expected damage is approximated very well by

$$\bar{d}(\bar{K},|h|) = \bar{K}\sqrt{\frac{1}{2\pi\bar{K}}} \exp\left[-\frac{h^2}{2\bar{K}}\right]. \tag{19}$$

Taking logarithms and inserting into Eq. (14) then yields the asymptotic scaling

$$\lim_{|h|\to\infty} K_c(|h|) = \frac{h^2}{2\ln|h|} \tag{20}$$

of the critical connectivity K_c. Figure 6 demonstrates the convergence of the critical line (straight-lined curve and data points) against this asymptote (dashed curve).

For finite $|h|$, we notice that there are substantial contributions from additional terms that vanish only logarithmically, and hence an approximation based on Eq. (20) would substantially underestimate K_c. This can be appreciated

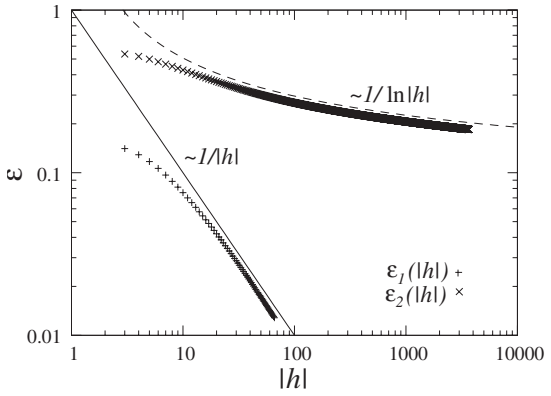

FIG. 7. Crosses (×): Relative error ε_1 between the approximation of Eq. (13) and the result obtained from the annealed approximation, as a function of $|h|$. For $|h| \geq 15$, ε_1 vanishes $\propto |h|^{-1}$; straight line with slope −1 shown for comparison. Data points (+): Relative error ε_2 between the approximation of Eq. (13) and the asymptotic scaling of Eq. (20); ε_2 goes to zero logarithmically (compare to dashed curve).

clearly from Fig. 7, which demonstrates the slow (logarithmic) convergence of the error $\varepsilon_2(|h|)$ made by application of Eq. (20) for finite $|h|$.

From Fig. 6, it is also evident that, for finite $|h|$, Eq. (20) overestimates the slope $dK_c/d|h|$. One can show that, for finite $|h|$, $K_c(|h|)$ is better approximated locally by power laws of the form

$$K_c(|h|) \approx a(|h|)|h|^{\alpha(|h|)} \tag{21}$$

with $3/2 < \alpha < 2$. We confirmed this intuition by numerically inserting candidate solutions with fixed α into Eq. (13), and solving for the values of $|h|$ and a where the deviation from the true curve $K_c(|h|)$ becomes minimal; inverting this relation, we obtain the optimal power law exponents $\alpha(|h|)$ as a function of $|h|$ (Fig. 8, for details, see Appendix E). Again, we can apply the Gaussian approximation for the damage propagation function to derive upper (lower) bounds for the

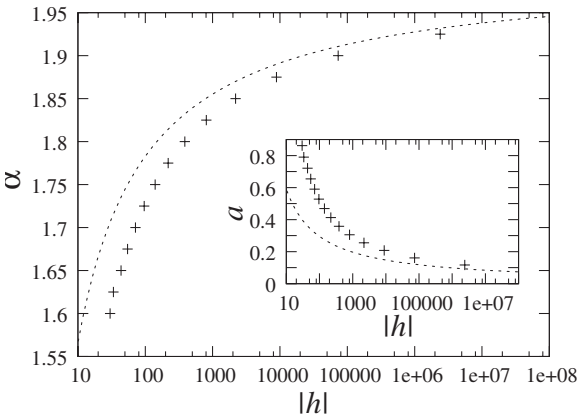

FIG. 8. Optimal exponents α of power laws $K_c \approx a|h|^{\alpha}$ that approximate the scaling function $K_c(|h|)$, as shown in Fig. 6, as a function of $|h|$. The dashed curves are the corresponding asymptotic estimates of Eqs. (22) and (23).

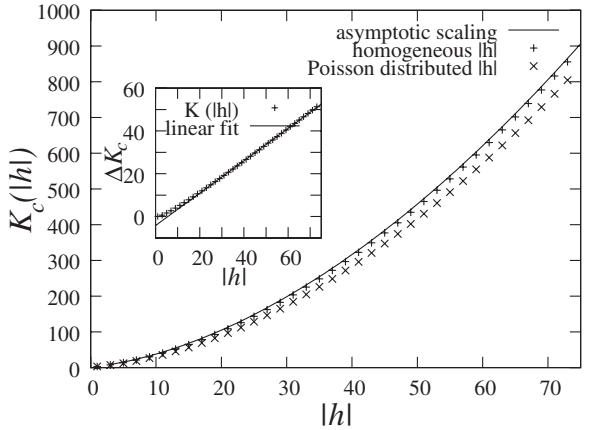

FIG. 9. $K_c(|h|)$ for homogeneous thresholds (+) and Poisson distributed thresholds with the same *average* $|\bar{h}|$ (×), annealed approximation. The solid line is the asymptotic scaling obtained from Eq. (14). For inhomogeneous $|h|$, the critical line is systematically below K_c of networks with homogeneous $|h|$. Inset: The difference $|\Delta K_c(|h|)|$ between both curves grows only linearly in $|h|$, confirming that the asymptotic scaling in the limit $|h| \to \infty$ is the same in both cases.

finite size scaling of $\alpha(|h|)$ and $a(|h|)$, which yield (cf. Appendix E)

$$\alpha(|h|) \approx 2 - \frac{1}{\ln|h|} \tag{22}$$

and

$$a(|h|) \approx \frac{e}{2\ln|h|}. \tag{23}$$

Figure 8 shows that the true optimal values are systematically below (α) or above (a) these curves, demonstrating the nontrivial scaling behavior of the critical line for finite $|h|$, which is significantly different from the simple asymptotic behavior in the thermodynamic limit [Eq. (20)].

Let us now investigate the scaling behavior of K_c for networks with inhomogeneous thresholds. Figure 9 shows that, for finite $|h|$, the critical line $K_c(|h|)$ for RTNs with inhomogeneous thresholds is always *below* the corresponding values for homogeneous $|h|$; the absolute *difference* $\Delta K_c(|h|) := |K_c^h(|h|) - K_c^i(|\bar{h}| = |h|)|$ between both curves, however, increases only linearly with $|h|$ (inset of Fig. 9), where $K_c^h(|h|)$ is the critical connectivity for homogeneous $|h|$, and $K_c^i(|\bar{h}|)$ is the corresponding value for inhomogeneously distributed $|h|$ with mean $|\bar{h}| = |h|$.

Intuitively, this is straightforward to understand: since we assumed that k and $|h|$ are *statistically independent*, $\Delta K_c(|h|)$ is determined solely by the *variance* σ_h^2 of the threshold distribution around the mean threshold $|\bar{h}| = |h|$—the smaller this variance is, the more peaked this distribution is around $|\bar{h}| = |h|$, and hence the less it differs from the homogeneous distribution. Since we assumed that (in the inhomogeneous case) thresholds are Poisson distributed around $|\bar{h}|$, we directly conclude

$$\Delta K_c(|h|) \sim \sigma_h^2 = |\bar{h}|. \tag{24}$$

For arbitrary threshold distributions that are statistically independent from the networks' degree distribution with variance σ_k^2, we make the ansatz

$$\sigma_{\text{tot}}^2 = \sigma_k^2 + \sigma_h^2 \tag{25}$$

for the total variance σ_{tot}^2. Using the same Gaussian approximation as above for the homogeneous case, one can show that

$$K_c(|\bar{h}|) \approx \frac{\bar{h}^2}{2\ln|\bar{h}|} - \sigma_h^2 \tag{26}$$

for networks with inhomogeneous thresholds distributed around an average absolute threshold $|\bar{h}|$ (for details, cf. Appendix C). This implies that, in the limit $|\bar{h}| \to \infty$, all networks with Poissonian distributed connectivity and threshold distributions with a variance which obeys the scaling relation $\sigma_h^2 \sim |\bar{h}|^\beta$ with $0 \leqslant \beta < 2$ follow the universal asymptotic scaling relation

$$K_c(|\bar{h}|) = \frac{\bar{h}^2}{2\ln|\bar{h}|}, \tag{27}$$

as it is shown in Appendix C. This means that in all these cases, the asymptotic scaling for $|\bar{h}| \to \infty$ is dominated by the scaling behavior of the maximum of the damage propagation function $p_s(k,|h|)$, with an exponent $\alpha=2$.

Let us now confirm this finding for a different class of threshold distributions. Since in a Poissonian the variance is not a free parameter, we now instead choose a discretized Gaussian distribution, i.e.,

$$P(|h|) = \frac{Z}{\sigma_h\sqrt{2\pi}} e^{-(1/2)(|h| - |\bar{h}|)^2/\sigma_h^2} \tag{28}$$

with

$$Z = \left\{ \sum_{|h|=0}^{|h|_{\text{m}}} \frac{1}{\sigma_h\sqrt{2\pi}} e^{-(1/2)(|h| - |\bar{h}|)^2/\sigma_h^2} \right\}^{-1} \tag{29}$$

and variance

$$\sigma_h^2 = |\bar{h}|^\beta, \quad \beta \in [0,\alpha). \tag{30}$$

The factor Z ensures that the probabilities are normalized in the interval $[0,|h|_m]$, where $|h|_{\text{m}}$ denotes the cutoff of the threshold distribution. Figure 10 compares the scaling functions $K_c(|\bar{h}|)$ for different values of β to the asymptotic case of homogeneous networks. Obviously, for finite $|\bar{h}|$, increased variance of the threshold distribution substantially lowers the critical connectivity; in the limiting case $\beta \approx \alpha$, K_c grows only linearly with $|\bar{h}|$. For $\beta < \alpha$, we find that the deviation from the scaling behavior of RTNs with homogeneous thresholds scales as

$$\Delta K_c \propto |\bar{h}|^{\beta_e}. \tag{31}$$

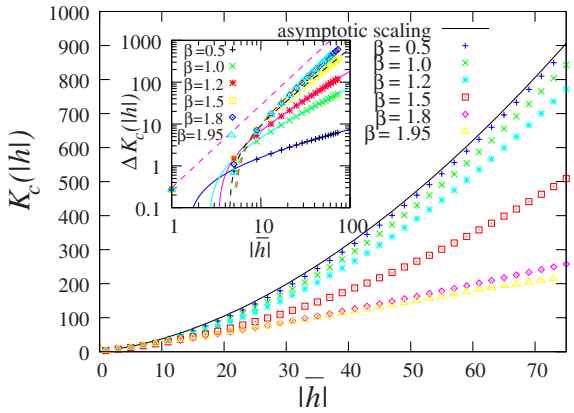

FIG. 10. (Color online) $K_c(\beta,|\bar{h}|)$ for networks with threshold distributions following discretized Gaussian distributions with different variances $\text{Var}(|h|)=|\bar{h}|^\beta$ (for details, see text). One clearly appreciates that the larger the variance of the threshold distribution, the more the curves $K_c(\beta,|\bar{h}|)$ are below the critical line of networks with homogeneous thresholds (blue solid line); in the limiting case $\beta=1.95\approx\alpha$ (yellow triangles), K_c scales almost linearly with $|\bar{h}|$. Inset: differences $|\Delta K_c(\beta,|\bar{h}|)|$ to the critical line of RTNs with homogeneous thresholds scale $\sim|\bar{h}|^{\beta_e}$ with $\beta<\beta_e<\alpha$ (power law fits and dashed line with slope α shown for comparsion); this implies asymptotic convergence to the universal scaling function Eq. (27) in the limit $|\bar{h}|\to\infty$ for all cases shown here.

Table I compares β and β_e (as obtained from fits of ΔK_c; in all cases, we have $\beta_e > \beta$, which is a discretization effect, but still $\beta_e < \alpha$. Hence it follows that

$$\lim_{|h|\to\infty} \frac{K_c(\beta,|\bar{h}|=|h|)}{K_c^{\text{h}}(|h|)} = \lim_{|h|\to\infty} \frac{K_c^{\text{h}}(|h|) - \Delta K_c(\beta,|h|)}{K_c^{\text{h}}(|h|)} = 1 - \text{const.} \lim_{|h|\to\infty} |h|^{\beta_e-\alpha} = 1 \tag{32}$$

for $\beta_e < \alpha$, i.e., in this case all scaling functions $K_c(\beta,|\bar{h}|)$ for $|h|\to\infty$ indeed asymptotically converge to the same universal scaling function, as given by Eq. (27).

Let us now have a closer look at the scaling behavior of the intersection points $K_{\text{d}}(|h|)$, as introduced in the last paragraph of Sec. III B. Let $\bar{d}^h(\bar{K},|h|)$ be the expected damage in networks with homogeneous threshold, and $\bar{d}^i(\bar{K},|\bar{h}|)$ the ex-

TABLE I. Scaling exponents β_e, as obtained from fits of $\Delta K_c \sim |\bar{h}|^{\beta_e}$, as a function of β.

β	β_e
0.5	0.533 ± 0.009
1.0	1.099 ± 0.004
1.2	1.327 ± 0.004
1.5	1.732 ± 0.004
1.8	1.942 ± 0.003
1.95	1.975 ± 0.004

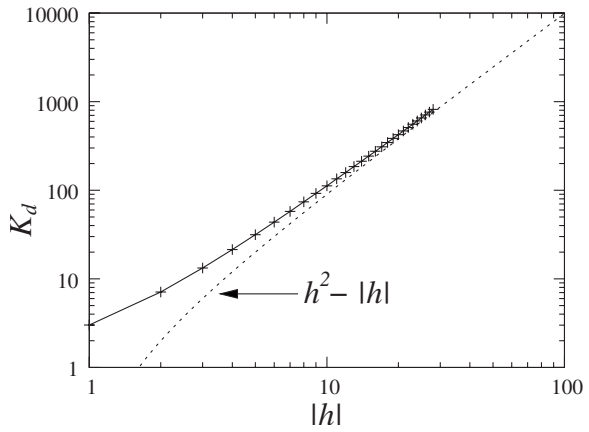

FIG. 11. Scaling behavior of $K_d(|h|)$ as a function of $|h|$, double logarithmic plot. The dashed line highlights the asymptotic scaling [Eq. (35)].

pected damage in networks with inhomogeneous thresholds; then

$$\bar{d}^{h}(K_d(|h|),|h|) - \bar{d}^{i}(K_d(|h|),|\bar{h}|) = 0, \tag{33}$$

$$|\bar{h}| = |h| \tag{34}$$

are the defining equations for $K_d(|h|)$. Notice that for $\bar{K} < K_d$, the randomness introduced by inhomogeneous thresholds actually *increases* the probability for damage spreading, whereas for $\bar{K} > K_d$, it is *decreased*. Equation (33), under condition Eq. (34), can be solved numerically for not to large $|h|$. Further, one can derive the asymptotic scaling in the thermodynamic limit by application of the Gaussian approximation for the damage propagation function (for details, cf. Appendix D), showing that

$$\lim_{|h|\to\infty} K_d(|h|) = h^2 - |h|. \tag{35}$$

Figure 11 demonstrates that $K_d(|h|)$ approaches this asymptotic scaling already for considerably small $|h|$, indicating that $K_d(|h|)$ is characterized by the same universal scaling exponent $\alpha=2$ as $K_c(|h|)$. Notice, however, that the asymptotic scaling law for K_d obeys a purely algebraic relation, whereas K_c has a dependence $\sim h^2/\ln|h|$ [Eq. (20)].

Let us briefly compare the scaling behavior of RTNs with nonzero thresholds, as discussed above, to random-Boolean networks (RBNs) with arbitrary transition functions not restricted to threshold-dependent switching. Obviously, increasing $|h|$ biases the output states of network nodes (for the systems discussed in this paper, it increases the probability to have an output state $\sigma_i=-1$). Biased RBNs obey the scaling relationship [41]

$$K_c = \frac{1}{2p(1-p)}. \tag{36}$$

To compare this relationship to the asymptotic scaling for RTNs in the limit of large $|h|$, we have to consider the limit $p \to 1$. One can show that, in this limit, the scaling function Eq. (36) logarithmically approaches the asymptotic scaling

$$K_c \approx -\frac{p^2}{2\ln p}. \tag{37}$$

This shows that $|h|$ plays the same role as the bias parameter p in RBNs, and that both classes obey the same scaling in the limit $p \to 1$ and $|h| \to \infty$, respectively. However, there are also substantial differences between both classes of systems, that come into play when $|h|$ is small (when p is close to $1/2$). In particular, while RBNs in this limit still obey the simple scaling relationship Eq. (36), the critical connectivity K_c of RTNs is derived from the complex dependence of Eq. (13). This difference is due to the fact that, in RTNs, local damage propagation strongly depends on the in-degree of nodes [cf. Eqs. (5) and (7)], while it is independent from the in-degree in RBNs for $k>0$. In the limit of sparsely connected networks (i.e., small $|h|$ and K_c), this leads to much stronger finite size effects in RTNs than in RBNs. Furthermore, in this limit also the absolute values of K_c in RTNs are considerably below those of RBNs [24,25].

Finally, let us remark on the existence of the characteristic connectivity K_d. As shown above, K_d is defined for RTNs with arbitrary $|h|$, in particular, it exists in the limit $|h| \to \infty$, with a well-defined asymptotic scaling. For biased RBNs, the corresponding limit is given by $p \to 1$ (or, equivalently, $p \to 0$). Obviously, we can in principle assign variable (inhomogeneous) biases p_i to different RBN nodes such that the *average* bias is equal to p. However, because p is a probability and hence $0 \leq p \leq 1$, the variance σ_p^2 has to vanish in the limit $p \to 1$ $(p \to 0)$ to yield a proper average bias. Since K_d is defined by comparing networks with diverging variance of the order parameter $|h|$ (or p, respectively) with the corresponding networks with vanishing variance and the same average $|h|$ (or p, respectively), this implies that K_d *is not defined for RBNs with arbitrary transition functions* in the limit of large bias $p \to 1$, which corresponds to $|h| \to \infty$ in RTNs. Hence K_d constitutes an interesting concept, yielding a different characteristic connectivity which is well-defined only for RTNs.

It is interesting to notice that the dependence of K_c, as well as of K_d on $|h|$, is clearly superlinear even for considerably small $|h|$; this has profound consequences for algorithms that evolve RTNs towards (self-organized) criticality by local adaptations of both thresholds and the number of inputs a node receives from other nodes [42]. In particular, it can be shown that co-evolution of network dynamics and thresholds or in-degrees leads to strong correlations between $|h|$ and k. To approach this type of problem analytically, we will now extend our analysis in this direction. first, In the next section, we will show that even weak correlations between k and $|h|$ can lead to a transition from subcritical to supercritical dynamics (and vice versa), while keeping the average connectivity $\bar{K}$ *and* the average absolute threshold $|\bar{h}|$ constant.

D. Effect of correlations between k and h

So far, we assumed that node degree and node thresholds are totally uncorrelated; while this matches well the "maximum disorder" assumption used in random ensemble based approaches as, e.g., the annealed approximation, this might

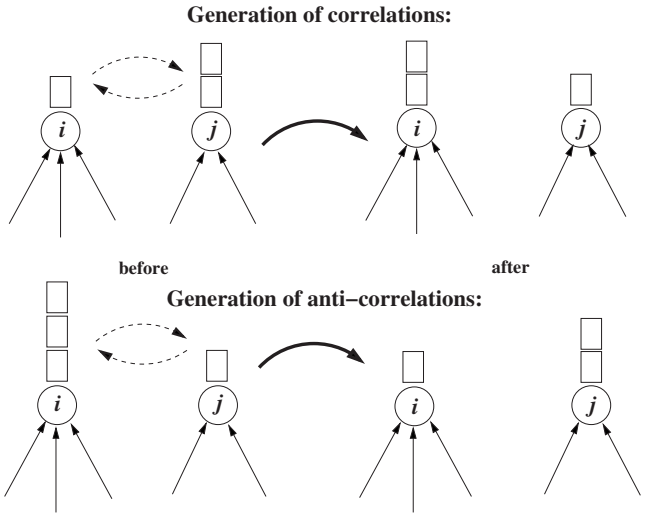

FIG. 12. Schematic illustration of the algorithm applied to generate local (anti)correlations between in-degree k_{in} and (absolute) threshold $|h|$. Arrows symbolize inputs from other nodes, boxes symbolize node thresholds (one box corresponds to $|h|=1$, two boxes to $|h|=2$, and so on). For details of the algorithm, please refer to the text.

be a quite unrealistic constraint for many real world networks. Indeed, one can show that even in a simple evolutionary algorithm that couples both the adaptation of node thresholds h_i and in-degree k_i to a local dynamical order parameter, strong correlations between both quantities emerge spontaneously [42]. Hence it is an interesting question to ask whether correlations (or anticorrelations) between h and k may induce a transition from subcritical to supercritical networks (or vice versa), while we keep $\bar{K}$ and $|\bar{h}|$ and network topologies constant.

Let us first formulate an algorithm that generates correlations (anticorrelations) between k and $|h|$. For this purpose, a parameter $c \in [0,1]$ is introduced which parametrizes the probability that k and $|h|$ are locally correlated (anticorrelated). The topology-generating algorithm then reads as follows (compare also Fig. 12):

(i) Generate a random, directed network with Poisson distributed k and Poisson distributed $|h|$ with average connectivity $\bar{K}$ and $|\bar{h}|$ for all sites.

(ii) Select a pair of sites $i \leqslant N$ and $j \leqslant N$ at random. $c > 0$: exchange the sites' thresholds if for the in-degrees $k(i) \geqslant k(j)$ holds, and for the thresholds $|h|(i) \leqslant |h|(j)$, or vice versa. $c < 0$: exchange the sites' thresholds if $k(i) \leqslant k(j)$ and $|h|(i) \leqslant |h|(j)$, or vice versa.

(iii) Go back to (ii) and repeat the algorithm for $c \times P_{\max}$ steps, where $P_{\max}$ is a predefined maximum number of correlated pairs.

Obviously, increasing the parameter $c \in [0,1]$ increases correlations (anticorrelations) between k and h. If we repeat this algorithm Z times for fixed c, we can generate a random ensemble of Z correlated or anticorrelated networks, and investigate damage spreading on these networks. The ensemble-averaged probability $\rho_c(k,|h|)$ to have a site with k inputs and threshold $|h_i|=|h|$ then is defined as

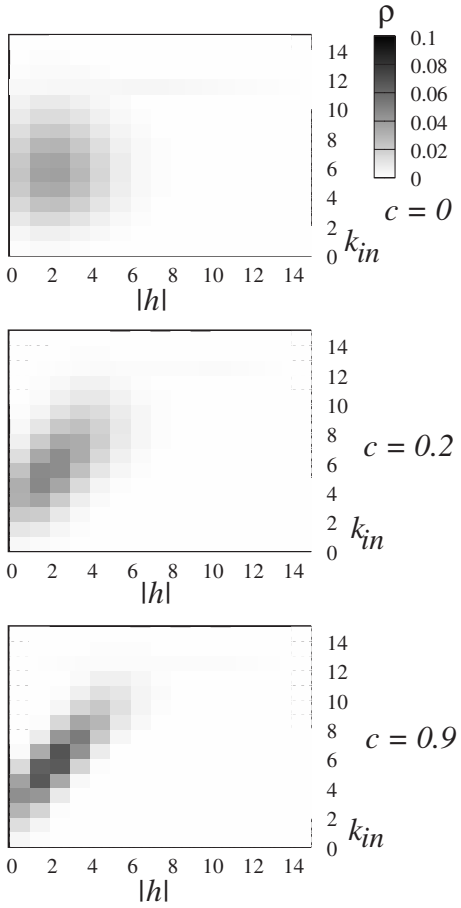

FIG. 13. Combined density $\rho(k_{\text{in}},|h|)$ for three different positive values of the correlation parameter c, from top to bottom: $c=0$, $c=0.2$, and $c=0.9$. Dark gray indicates a high probability density. The diagonal structure of $\rho(k_{\text{in}},|h|)$ for $c=0.9$ (lower panel) indicates emergence of strong positive correlations between k_{in} and $|h|$.

$$\rho_c(k,|h|) = \frac{\Sigma_{j=1}^{Z} n_j(k,|h|)}{ZN}, \tag{38}$$

where $n_j(k,|h|)$ is the number of sites with k inputs and threshold $|h_i|=|h|$ in the jth random network. Figure 13 demonstrates the correlating effect of the algorithm on the *average* probabilities $\rho_c(k,|h|)$ for ensembles of 10^5 randomly generated networks, for the case $c \geqslant 0$, with $P_{\max}=10^4$. For $c=0$, clearly no correlations are present, and the combined density simply represents the independent superposition of the two underlying Poisson distributions. With increasing c, correlations gradually emerge, and for $c=0.9$ the resulting distribution clearly exhibits a diagonal structure. Figure 14 demonstrates the corresponding effect for $c \leqslant 0$, i.e., anticorrelated topologies.

Let us now investigate how these correlations affect damage propagation. In a finite network of size N, the expected damage at time step $t=1$, after a one-bit perturbation at $t=0$, is given by

$$\bar{d}(t+1) = \sum_{|h|=0}^{|h|_{\text{m}}} \sum_{k=|h|}^{N} k \rho_c(k,|h|) p_s(k,|h|), \tag{39}$$

with the normalization conditions

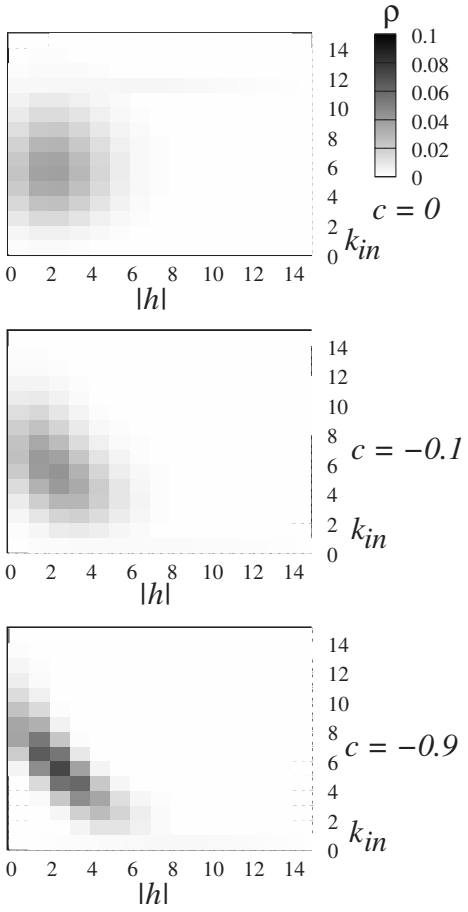

FIG. 14. Combined density $\rho(k_{in},|h|)$ for three different negative values of the correlation parameter c, from top to bottom: $c=0$, $c=-0.1$, and $c=-0.9$. Dark gray indicates a high probability density. The inverted diagonal structure of $\rho(k_{in},|h|)$ for $c=-0.9$ (lower panel) indicates emergence of strong anticorrelations between k_{in} and $|h|$.

$$\sum_{|h|=0}^{|h|_{\mathrm{m}}} \sum_{k=|h|}^{N} \rho_c(k,|h|) = 1 \tag{40}$$

and

$$\sum_{|h|=0}^{|h|_{\mathrm{m}}} \sum_{k=|h|}^{N} |h| \rho_c(k,|h|) = |\bar{h}|, \tag{41}$$

where $|h|_{\mathrm{m}}$ is the maximal absolute threshold observed (cutoff); correlations enter via the probabilities $\rho_c(k,|h|)$ to observe a node with in-degree k and absolute threshold $|h|$ for a given value of c.

Figure 15 compares the numerically observed damage $\bar{d}$ (for ensembles of randomly generated networks) one time step after a one-bit perturbation to the expected damage, as predicted by the annealed approximation according to Eq. (39) (lined curves). While all other parameters that characterize network topology, namely $\bar{K}$ and $\bar{h}$, are held constant, increasing the probability of positive correlations between in-degree and thresholds (i.e., $|h_i| \propto k_i$) leads to a transition from supercritical ($\bar{d}>1$) to subcritical ($\bar{d}<1$) dynamics.

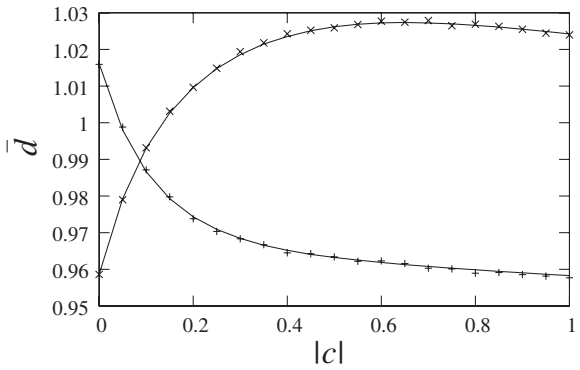

FIG. 15. Average damage $\bar{d}(c)$ as a function of $|c|$, for correlated k_{in} and $|h|$ (+) and anticorrelated k_{in} and $|h|$ (×), with $\bar{K}=6.15$ for $c \geqslant 0$ networks, $\bar{K}=5.8$ for $c \leqslant 0$ networks, and $|\bar{h}|=2.5$ in both cases. Numerical data were obtained from ensemble averages over $Z=5\times10^5$ randomly generated RTNs with $N=1024$ nodes for each data point. Solid curves are the corresponding results of the annealed approximation.

The opposite effect is observed when the probability for anticorrelations ($c<0$) is increased. This observation constitutes an interesting mechanism for a transition from ordered to chaotic dynamics (and vice versa) in discrete dynamical networks. When we consider larger initial perturbation sizes, and plot the temporal evolution of the *relative* average damage $y(t) := \bar{d}(t)/N$, the effect of correlations on damage supression becomes even more evident (Fig. 16); for networks with $\bar{K}=6.15$, $\bar{h}=-2.5$, and $N=1024$, for example, increasing c from zero to one has the same effect as lowering the average connectivity to $\bar{K}=5.85$ (Fig. 16, inset), i.e., removing about 300 links from the network.

Last, let us investigate how (anti)correlations between input number and thresholds change the *variance* σ_d^2 of the damage, which in the one-step approximation is given by

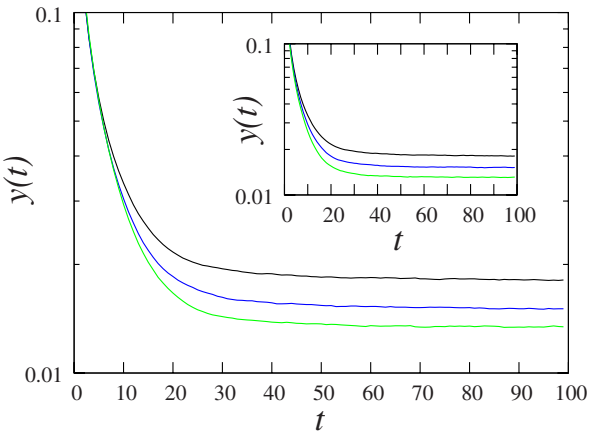

FIG. 16. (Color online) Relative damage $y(t)=\bar{d}(t)/N$ at time t after an initial perturbation $y(0)=0.3$, for three different values of c (from top to bottom: $c=0$, $c=0.15$, and $c=1.0$). Data were averaged over 10^4 network realizations with $N=1024$, $\bar{K}=6.15$, and $\bar{h}=-2.5$. Inset: the same for constant $c=0$ and $\bar{h}=-2.5$ and variable $\bar{K}$, from top to bottom: $\bar{K}=6.15$, $\bar{K}=6.0$, and $\bar{K}=5.85$.

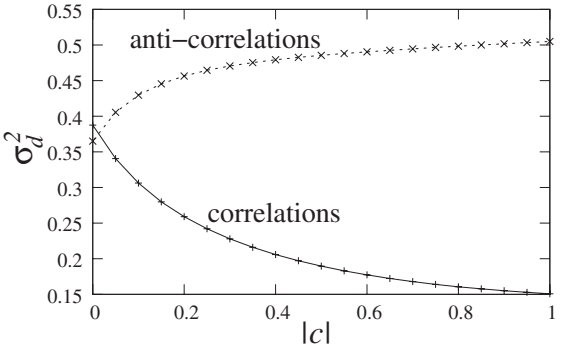

FIG. 17. Variance σ_d^2 of the damage one time step after a one-bit perturbation, for correlated k and h (i.e., $c>0$) and anticorrelated k and h, as indicated. For $c>0$, $\bar{K}=6.15$ was applied, for $c<0$, $\bar{K}$ was set to 5.8, with $\bar{h}=-2.5$ in both cases.

$$\sigma_d^2 = \sum_{|h|=0}^{|h|_m} \sum_{k=|h|}^{N} [kp_s(k,|h|) - \bar{d}(t+1)]^2 \rho_c(k,|h|). \quad (42)$$

The dependence of σ_d^2 on $|c|$ is shown for correlations ($c>0$) and anticorrelations ($c<0$) in Fig. 17. Positive c values lead to a significant reduction of the variance, while it is only moderately increased by negative values of c. This suggests that positive correlations between k and $|h|$ not only lower the *average* damage, but also lead to a quite strong suppression (and hence better control) of *extreme* damage events. Possible relations of these observations to gene regulatory networks will be discussed in the following section.

IV. DISCUSSION

An increasing number of studies is concerned with the propagation dynamics of perturbations and/or information in complex dynamical networks. Discrete dynamical networks, in particular random-Boolean networks (RBNs) and random-threshold networks (RTNs), constitute an ideal testbed for this type of question, since they are easily accessible for both computational methods and the tool boxes of statistics and combinatorics. Often, it is found that damage or information propagation strongly depends on the type of inhomogeneities present in network wiring. Several studies focus, for example, on the effect of scale-free degree distributions [25,26]. Typically, these studies employ mean-field methods and hence represent, in a sense, strongly idealized models, since they derive results that strictly hold in the thermodynamic limit only.

Consequently, a second line of research concentrates on modification of damage propagation due to finite-size effects, which play a decisive role in many real-world networks. Recently, it was shown that weakly perturbed, finite size RBNs and RTNs show pronounced deviations from the annealed approximation [11]. Fronczak and Fronczak showed that these deviations can be explained by inhomogeneities and emergent correlations found at the percolation transition [43], however, their study is currently limited to undirected networks. In this context, the system discussed in our paper constitutes a complementary approach: it allows us to introduce *dynamical inhomogeneity* of network units, without otherwise altering network topology. While this type of dynamical diversity certainly plays an important role in many real-world networks, it is neglected by most researchers. Let us now briefly summarize the main results of our study.

We studied damage propagation in random-threshold networks (RTNs) with homogeneous and inhomogeneous negative thresholds, both analytically (using an annealed approximation) and in numerical simulations. We derived the probability $p_s(k,|h|)$ of damage propagation for arbitrary in-degree k and (absolute) threshold $|h|$ [Eqs. (4)–(7)], and, from this, the corresponding *annealed* probabilities $\langle p_s \rangle$ [Eqs. (9) and (11)] and the expected damage $\bar{d}$ [Eq. (12)], for both the cases of homogeneous and inhomogeneously distributed thresholds. On these grounds, we investigated the scaling behavior of the critical connectivity K_c as a function of $|h|$. Using a mean field approximation, a simplified scaling equation for the logarithm of the average damage was derived [Eq. (13)], and applied to derive the critical line $K_c(|h|)$ (Fig. 6). It was shown that this function exhibits a superlinear increase with $|h|$, which asymptotically approaches a unique scaling law $K_c(|h|) \sim h^2/(2\ln|h|)$ for large $|h|$ [Eq. (20) and Fig. 7]. However, convergence against this asymptotic scaling is very slow (logarithmic in $|h|$), which indicates that finite size effects are very dominant, and cannot be neglected for realistically sized networks. We presented evidence that this asymptotic scaling is universal for RTNs with Poissonian distributed connectivity and threshold distributions with a variance that grows slower than h^2, for both the cases of Poisson distributed thresholds (Fig. 9) and thresholds distributed according to a discretized Gaussian (Fig. 10). Interestingly, inhomogeneity in thresholds, meaning that each site has an individual threshold $|h_i|$ drawn, e.g., from a Poisson distribution with mean $|\bar{h}|$, increases damage for small average connectivity $\bar{K}$, when compared to homogeneous networks with the same average threshold $|h|=\bar{h}$, whereas for larger $\bar{K}$ with $\bar{K}>K_d$, damage is reduced. This establishes a new characteristic connectivity $K_d(|h|)$ with $K_d>K_c$, that describes the ambivalent effect of threshold inhomogeneity on RTN dynamics. We showed that $K_d(|h|)$ asymptotically converges against a unique scaling law $K_d \sim h^2$ in the limit $|h|\to\infty$. The scaling of K_d was compared to the corresponding case of random-Boolean networks (RBNs) with arbitrary transition functions not restricted to threshold-dependent switching and with inhomogeneously distributed bias, parametrized in terms of a bias parameter $1/2 \leqslant p \leqslant 1$. It was shown that K_d *is not defined for RBNs* in the limit $p \to 1$, which corresponds to $|h|\to\infty$ in RTNs. Hence K_d yields a different characteristic connectivity for RTNs. In light of the fact that, in the past, similarities or correspondences between RBNs and RTNs were strongly emphasized [23], and, correspondingly, both types of dynamical networks were used in many studies concerned with models of biological networks in an almost interchangeable way, these observations might be of considerable interest for future studies. They might also affect other generalizations of RTNs studied in the statistical physics community, e.g., networks with probabilistic update of units [25].

Last, we introduced local correlations between in-degree k_{in} of network nodes and their (absolute) threshold $|h|$, while

keeping all other network parameters constant. We found that even small positive correlations can induce a transition from supercritical (chaotic) to subcritical (ordered) dynamics, while anticorrelations have the opposite effect. Further, positive correlations significantly reduce the variance of the damage size distribution, which suggests that extreme damage events are suppressed, and hence better controlled. A number of interesting questions arise for future extensions of this research, namely, the possibility that the introduced dependencies between thresholds of neighboring nodes may lead to interesting deviations from the annealed approximation in the dynamics after multiple time steps. Similar deviations have been discovered in other contexts in several recent studies [11,43,44], demonstrating the need for an extended theory that takes into account dynamical correlations as well as local structure in network topology. Theoretical approaches to these problems are faced with many new challenges, in particular, they will have to account for the complex (and far from random) structure of state space after multiple dynamical updates and modification of damage propagation by a bias towards ON or OFF states [45]. Further, the proposed threshold-swapping algorithm can be easily extended to introduce local internode correlations that are not present in ordinary random networks, and hence might reveal interesting new insights that could be highly relevant to systems theory in general.

To summarize, dynamics of damage (or information) propagation in RTNs with inhomogeneous thresholds and Poisson distributed connectivity shows both similarities and differences, when compared to networks with homogeneous thresholds: similarities manifest themselves in common universal scaling functions for both K_c and K_d, whereas differences show up in the opposite effects of threshold inhomogeneity for small and large $\bar{K}$. Differences become even more prominent in networks that are characterized by correlations between in-degree and thresholds; here, the probability for correlations defines a new control parameter for global network dynamics. Let us now outline how the results achieved in this study could be relevant for models of real world dynamical networks.

In recent years, for example, a number of studies have been published that model the dynamics of gene regulatory dynamics with RTNs (e.g., [34–36]). In most cases, the switching behavior of regulatory units is assumed to depend only on network wiring. Our results indicate that, while general characteristics as, for example, the scaling behavior of critical points may be conserved in approximations of this type, inhomogeneous thresholds can strongly impact the details of network dynamics, and hence should be taken into account in models that aim to give a realistic description of the dynamics of regulatory networks. Furthermore, context-dependent "reprogramming" of thresholds might serve as a first approximation for the ubiquitous reprogramming of gene regulatory networks in Eukaryotes by other (and more flexible) mechanisms than rewiring of transcriptional regulatory interactions, for example through the effects of microRNA [31–33] and gene silencing by DNA methylation [46], which contribute significantly to both robustness and flexibility of these biological networks.

ACKNOWLEDGMENTS

The author thanks A. Hübler for interesting discussions and careful reading of the manuscript, and acknowledges significant contributions of an anonymous referee with regard to the discussion of scaling behavior.

APPENDIX A: DERIVATION OF $p_s(k,|h|)$

In this section, we provide a derivation of the local damage propagation probability $p_s(k,|h|)$.

Consider a network site i with k inputs; k_+ of these have positive sign, k_- negative sign, hence $k_+ + k_- = k$. We now derive the conditions under which a inversion of one input spin at time t leads to a switch of the output of site i at time $t+1$.

(i) $k-|h|$ odd: From Eqs. (1) and (2) it is easy to see that input-spin flips produce "damage" only if one of the following conditions holds:

$$k_+ - k_- - |h| = 1 \tag{A1}$$

or

$$k_+ - k_- - |h| = -1. \tag{A2}$$

In case (A1), only the reversal of positive spins is effective, whereas in case (A2), only the reversal of negative spins has an effect. We have

$$k_+ = \frac{k + |h| + 1}{2} \tag{A3}$$

in the first case and

$$k_- = \frac{k - |h| + 1}{2} \tag{A4}$$

in the second case. There is a total number of $k2^k$ possible spin configurations, of which $\binom{k}{(k+|h|+1)/2}$ fulfill condition (A3) and $\binom{k}{(k-|h|+1)/2}$ fulfill condition (A4). Hence the damage propagation probability follows as

$$p_s(k,|h|) = k^{-1}2^{-(k+1)}\left[(k+|h|+1)\binom{k}{\frac{k+|h|+1}{2}} + (k-|h|+1)\binom{k}{\frac{k-|h|+1}{2}}\right] \tag{A5}$$

$$= \frac{2^{-(k-1)}(k-1)!}{[(k+|h|-1)/2]![(k-|h|-1)/2]!} \tag{A6}$$

$$= 2^{-(k-1)}\binom{k-1}{\frac{k+|h|-1}{2}}. \tag{A7}$$

(ii) $k-|h|$ even: Here, we have as necessary conditions

$$k_+ - k_- - |h| = 0 \tag{A8}$$

or

$$k_+ - k_- - |h| = 2. \tag{A9}$$

In the first case, only the reversal of negative spins is effective, whereas in the latter case the same holds for positive spins. We have

$$k_- = \frac{k - |h|}{2} \tag{A10}$$

in the first case and

$$k_+ = \frac{k + |h| + 2}{2} \tag{A11}$$

in the second case. There is a total number of $k2^k$ possible spin configurations, of which $\binom{k}{(k-|h|)/2}$ fulfill condition (A10) and $\binom{k}{(k+|h|+2)/2}$ fulfill condition (A11). Hence the damage propagation probability follows as

$$p_s(k,|h|) = k^{-1}2^{-(k+1)}\left[(k-|h|)\binom{k}{\frac{k-|h|}{2}} + (k+|h|+2)\binom{k}{\frac{k+|h|+2}{2}}\right] \tag{A12}$$

$$= \frac{2^{-(k-1)}(k-1)!}{[(k-|h|-2)/2]![(k+|h|)/2]!} \tag{A13}$$

$$= 2^{-(k-1)}\binom{k-1}{\frac{k+|h|}{2}}. \tag{A14}$$

APPENDIX B: ANNEALED APPROXIMATION FOR DAMAGE PROPAGATION

Assuming that input states are drawn uniformly at random such that $\sigma_i = +1$ and $\sigma_i = -1$ with equal probability, the expected damage at a randomly picked node with k inputs one time step after a one-bit spin flip at time t is given by

$$\bar{d}(t+1) = \sum_{k=|h|}^{\infty} k\rho_k p_s(k,|h|), \tag{B1}$$

taking into account that the probability of a node to become damaged is proportional to its number of inputs k and its damage propagation probability $p_s(k,|h|)$. Assuming *uniform link selection*, the probability that a randomly chosen link propagates damage follows as

$$\langle p_s\rangle(\bar{K},|h|) = \frac{\bar{d}}{\bar{K}} = \frac{1}{\bar{K}}\sum_{k=|h|}^{\infty} k\rho_k p_s(k,|h|), \tag{B2}$$

and hence

$$\bar{d}(t+1) = \langle p_s\rangle(\bar{K},|h|)\bar{K}. \tag{B3}$$

Let us now apply Eq. (B2) to networks with Poisson distributed connectivity and constant $|h|$. With $\rho_k = (\bar{K}^k/k!)e^{-\bar{K}}$, it follows that

$$\langle p_s\rangle(\bar{K},|h|) = \frac{e^{-\bar{K}}}{\bar{K}}\sum_k k\frac{\bar{K}^k}{k!}p_s(k,|h|) = e^{-\bar{K}}\sum_k \frac{\bar{K}^{k-1}}{(k-1)!}p_s(k,|h|)$$

$$= e^{-\bar{K}}\sum_k \frac{\bar{K}^k}{k!}p_s(k+1,|h|), \tag{B4}$$

which is identical with Eq. (15) in Ref. [24] for the case $|h|=0$. In the last step, the summation index k was shifted by 1, which does not affect the results as $p_s(k,|h|)=0$ for all $k \leqslant |h|$. We would like to mention that page 250 of Ref. [24] provides a different and incorrect reasoning leading to Eq. (B4), not taking into account that the average in $\langle p_s\rangle$ is defined for uniform link selection rather than uniform node selection, which may lead to wrong conclusions.

Let us briefly discuss the range of applicability of relation (B4). In a one-step annealed approximation as given by Eq. (B3), it provides a correct description of damage propagation. In a generalization to larger times, however, considerable care has to be taken. In particular, in Ref. [24] the following recursive map for the relative damage y_{t+1} at time $t+1$ is provided:

$$y_{t+1} = \langle p_s\rangle(\bar{K})\sum_k \rho_k[1-(1-y_t)^k] \tag{B5}$$

This map provides a good approximation for small $\bar{K}$ and for large N, and when a relatively homogeneous distribution of connectivity is present (compare Fig. 3 in Ref. [24]). In particular, it provides a critical connectivity K_c consistent with the results of the one-step annealed approximation for the case $|h|=0$ in networks with Poissonian distributed ρ_k (Fig. 4 in Ref. [24], and discussion on page 253 in the same paper). However, in general Eq. (B5) cannot be applied for arbitrary topologies and larger $|h|$; in this case, the dependence of the probability of damage propagation on k and $|h|$ requires a more complicated mean field calculation of y_{t+1}. This will be discussed in more detail in a separate publication.

APPENDIX C: DERIVATION OF THE SCALING EQUATION

For RTNs with Poisson distributed in- and out-degree, the critical line is given by the condition

$$\bar{d}(t+1) = \langle p_s\rangle(K_c(|h|),|h|)K_c(|h|) = 1 \tag{C1}$$

with

$$\langle p_s\rangle(\bar{K},|h|) = e^{-\bar{K}}\sum_{k=|h|}^{N}\frac{\bar{K}^k}{k!}p_s(k+1,|h|). \tag{C2}$$

Instead of averaging over the ensemble of all possible network topologies as in Eq. (C2), we now make an explicit *mean field approximation*, and consider a "typical" network

node with $k \approx \bar{K}$ inputs. Consequently, we approximate

$$\langle p_s \rangle(\bar{K}, \overline{|h|}) \approx p_s(\lfloor \bar{K} \rfloor, |h|), \tag{C3}$$

where $\lfloor . \rfloor$ denotes the floor function. In the limit of large $\bar{K}$ and $|h|$, the difference between the damage propagation probabilities for even and odd k vanishes, i.e., we can set

$$\langle p_s \rangle(\bar{K}, \overline{|h|}) \approx 2^{-(\lfloor \bar{K} \rfloor - 1)} \binom{(\lfloor \bar{K} \rfloor - 1)}{\frac{\lfloor \bar{K} \rfloor + |h|}{2}}, \tag{C4}$$

and hence, under the condition that $\bar{K} \ll |h|$, we can approximate

$$\bar{d}(\bar{K}, |h|) \approx \bar{K} 2^{-\lfloor \bar{K} \rfloor} \binom{\lfloor \bar{K} \rfloor}{\frac{\lfloor \bar{K} \rfloor + |h|}{2}} \tag{C5}$$

without loss of generality.

Using the Stirling approximation $n! \approx n^n e^{-n} \sqrt{2\pi n}$, dropping the floor function (since we now consider a function of real-valued variables only) and taking logarithms, we obtain

$$\ln[\bar{d}(\bar{K}, |h|)] \approx \ln \bar{K} - \ln 2\bar{K} + Z_1 - Z_2 - Z_3 \tag{C6}$$

with

$$Z_1 = \ln[\bar{K}^{\bar{K}} e^{-\bar{K}} \sqrt{2\pi\bar{K}}],$$

$$Z_2 = \ln\left[\left(\frac{\bar{K} - |h|}{2} \right)^{(\bar{K} - |h|)/2} e^{-(\bar{K} - |h|)/2} \sqrt{\pi(\bar{K} - |h|)} \right]$$

and

$$Z_3 = \ln\left[\left(\frac{\bar{K} + |h|}{2} \right)^{(\bar{K} + |h|)/2} e^{-(\bar{K} + |h|)/2} \sqrt{\pi(\bar{K} + |h|)} \right].$$

Summing out the logarithms in Z_1, Z_2, and Z_3, one realizes that all terms linear in $\bar{K}$ drop out, resulting in

$$\ln[\bar{d}(\bar{K}, |h|)] \approx \ln \bar{K} + \left(\bar{K} - \frac{1}{2} \right) \ln \bar{K} - \frac{\bar{K} - |h| + 1}{2} \ln(\bar{K} - |h|) - \frac{\bar{K} + |h| + 1}{2} \ln(\bar{K} + |h|) + C \tag{C7}$$

with $C = \ln(\sqrt{2/\pi})$. Using some simple algebra and approximating $|h| + 1 \approx |h|$, this can be reformulated as

$$\ln[\bar{d}(\bar{K}, |h|)] \approx \ln \bar{K} - \frac{1}{2} \left\{ \ln(\bar{K} - \bar{K} \ln\left[\frac{(\bar{K} + |h|)(\bar{K} - |h|)}{\bar{K}^2} \right] + |h| \ln\left[\frac{\bar{K} + |h|}{\bar{K} - |h|} \right] \right\} + C. \tag{C8}$$

This leads to the final result,

$$\ln[\bar{d}(\bar{K}, |h|)] \approx \frac{1}{2} \left\{ \ln \bar{K} - \bar{K} \ln\left[1 - \left(\frac{|h|}{\bar{K}} \right)^2 \right] - |h| \ln\left[\frac{\bar{K} + |h|}{\bar{K} - |h|} \right] \right\} + C. \tag{C9}$$

APPENDIX D: ASYMPTOTIC SCALING OF K_c

Let us now derive the asymptotic scaling behavior of the critical connectivity $K_c(|h|)$. We start with the case of homogeneous thresholds, and then generalize to inhomogeneous thresholds.

First, we note that the right-hand side of Eq. (C5) has the form of a binomial distribution,

$$P(n,k) = \binom{n}{k} p^n q^{n-k}, \tag{D1}$$

with $p = q = 1/2$, $n = \lfloor \bar{K} \rfloor$, and $k = (\lfloor \bar{K} \rfloor + |h|)/2$, multiplied with a prefactor $\bar{K}$. In the limit $\bar{K} \to \infty$ and $|h| \to \infty$, we can replace the binomial distribution with a Gaussian and drop the floor function, i.e.,

$$\bar{d}(\bar{K}, |h|) = \bar{K} C_n \exp\left[- \frac{((\bar{K} + |h|)/2 - \bar{K}/2)^2}{2\bar{K}(1/2)(1/2)} \right]. \tag{D2}$$

This simplifies to

$$\bar{d}(\bar{K}, |h|) = \bar{K} \sqrt{\frac{1}{2\pi\bar{K}}} \exp\left[- \frac{h^2}{2\bar{K}} \right] \tag{D3}$$

with the normalization constant $C_n = \sqrt{1/(2\pi\bar{K})}$ and variance $\sigma^2 = \bar{K}$.

In the case of inhomogeneous thresholds, we can still use this approximation, however, the variance σ_h^2 of the threshold distribution adds to the variance of the damage propagation function of the homogeneous case. This implies that we have to replace $\bar{K}$ with $\bar{K} + \sigma_h^2$, and hence

$$\bar{d}(\bar{K}, |\bar{h}|) = \frac{\bar{K} + \sigma_h^2}{\sqrt{2\pi(\bar{K} + \sigma_h^2)}} \exp\left[- \frac{\bar{h}^2}{2(\bar{K} + \sigma_h^2)} \right]. \tag{D4}$$

To obtain the criticality condition, we take logarithms and set the result to zero, leading to

$$\ln[K_c + \sigma_h^2] - \frac{1}{2} \ln[2\pi(K_c + \sigma_h^2)] - \frac{\bar{h}^2}{2(K_c + \sigma_h^2)} = 0. \tag{D5}$$

This simplifies to

$$\bar{h}^2 = (K_c + \sigma_h^2) \ln\left[\frac{K_c + \sigma_h^2}{2\pi} \right]. \tag{D6}$$

To solve this equation with respect to K_c, we make the ansatz

$$K_c + \sigma_h^2 \approx \frac{\bar{h}^2}{2\ln|\bar{h}|}. \tag{D7}$$

Inserting for $K_c+\sigma_h^2$ into Eq. (D6), we obtain

$$\bar{h}^2 \approx \frac{\bar{h}^2}{2\ln|\bar{h}|}\ln\left[\frac{\bar{h}^2}{4\pi\ln|\bar{h}|}\right] \tag{D8}$$

$$= \bar{h}^2\left\{1 - \frac{\ln[4\pi\ln|\bar{h}|]}{2\ln|\bar{h}|}\right\}. \tag{D9}$$

Since the second term in the bracket vanishes logarithmically for $|\bar{h}|\to\infty$, we have verified that Eq. (D7) yields the correct asymptotic scaling. Consequently, the asymptotic scaling of the critical line for large $|\bar{h}|$ is given by

$$K_c\left(|\bar{h}|\right) \approx \frac{\bar{h}^2}{2\ln|\bar{h}|}\Bigg) - \sigma_h^2. \tag{D10}$$

However, notice that the convergence is very slow, as can be appreciated from the logarithmic finite-size term in Eq. (D9). In particular, we conclude that the asymptotic scaling for networks with homogeneous thresholds, i.e., $|h|=$const and $\sigma_h=0$ is given by

$$K_c^{\mathrm{hom}}(|h|) \approx \frac{h^2}{2\ln|h|}. \tag{D11}$$

Let us now prove that this scaling is universal for $|\bar{h}|\to\infty$ for all threshold distributions possessing a variance $\sigma_h^2\sim|\bar{h}|^\alpha$ with $0\leqslant\alpha<2$. In this case, we have

$$\lim_{|h|\to\infty}\frac{K_c(|\bar{h}|)}{K_c^{\mathrm{hom}}(|h|)} = \lim_{|h|\to\infty}\frac{K_c^{\mathrm{hom}}(|h|)-\sigma_h^2}{K_c^{\mathrm{hom}}(|h|)} \tag{D12}$$

$$= 1 - \lim_{|h|\to\infty}\frac{\sigma_h^2}{K_c^{\mathrm{hom}}(|h|)} \tag{D13}$$

$$= 1 - \lim_{|h|\to\infty}\frac{2\ln|h||h|^\alpha}{h^2} \tag{D14}$$

$$= 1 - \lim_{|h|\to\infty}\frac{2\ln|h|}{|h|^{2-\alpha}}. \tag{D15}$$

Since we assumed $0\leqslant\alpha<2$, the limit in Eq. (D15) vanishes, and hence the asymptotic scaling equation (D11) is indeed universal for this class of threshold distributions.

APPENDIX E: ASYMPTOTIC SCALING OF K_d

The characteristic connectivity K_d is defined by the conditions

$$|h| = |\bar{h}|, \tag{E1}$$

where $|h|$ is the (constant) threshold of a homogeneous network, and $|\bar{h}|$ is the average threshold of a corresponding network with inhomogeneous thresholds, and

$$\bar{d}^h(K_d(|h|),|h|) - \bar{d}^i(K_d(|h|),\overline{|h|}) = 0, \tag{E2}$$

where $\bar{d}^h$ is the expected damage for homogeneous networks, and $\bar{d}^i$ is the expected damage for inhomogeneous networks. Let us further assume that thresholds are Poissonian distributed, i.e., $\sigma_h^2=|h|$. If we apply the same Gaussian approximation as in Appendix D, these conditions lead to

$$\frac{e^{-h^2/(2K_d)}}{\sqrt{2\pi K_d}} = \frac{e^{-h^2/(2(K_d+|h|))}}{\sqrt{2\pi(K_d+|h|)}}. \tag{E3}$$

Taking logarithms and reordering, this reduces to

$$\ln\left[\frac{K_d+|h|}{K_d}\right] - \frac{h^2}{K_d} + \frac{h^2}{K_d+|h|} = 0. \tag{E4}$$

Linearization of the first term leads to the approximation

$$\frac{|h|}{K_d} - \frac{h^2}{K_d} + \frac{h^2}{K_d+|h|} \approx 0. \tag{E5}$$

Solving this equation for K_d finally yields the asymptotic scaling

$$K_d(|h|) \approx h^2 - |h|, \tag{E6}$$

i.e., K_d scales quadratically with $|h|$.

APPENDIX F: POWER-LAW APPROXIMATION OF $K_c(|h|)$ FOR FINITE $|h|$

In this section, we first describe how to identify numerically candidate solutions (power laws)

$$K_c(|h|) \approx a(|h|)|h|^{\alpha(|h|)} \tag{F1}$$

that optimally approximate Eq. (13) for finite (critical) $|h|_c$.

We start with a fixed $\alpha\in[1.6,2)$ and define

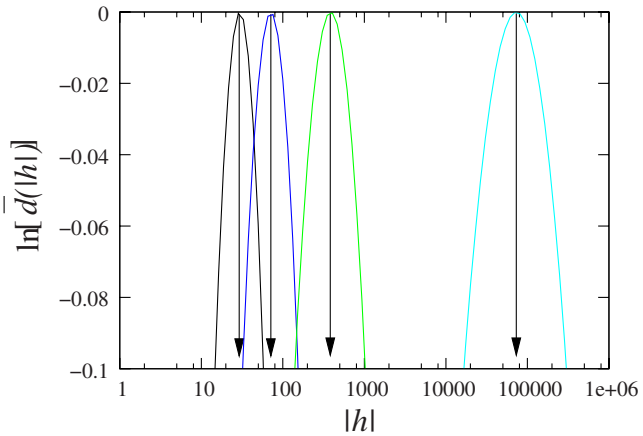

FIG. 18. (Color online) Solutions of Eq. (F3) for (from the left to the right) $\alpha=1.6$, $\alpha=1.7$, $\alpha=1.8$, and $\alpha=1.9$. Projections of the maximum on the $|h|$ axis (as indicated by arrows) yield the corresponding values of $|h|_c$ at which the approximations are optimal.

$$F(y) := \frac{1}{2}\left\{ \ln y - y\ln\left[1 - \left(\frac{|h|}{y} \right)^2 \right] - (|h|+1)\ln\left[\frac{y+|h|}{y-|h|} \right] \right\} + C \tag{F2}$$

with $y=a|h|^{\alpha}$. One can show that, for any finite a and α, $F(y)$ has a maximum at a finite value $|h|_{\max}$. We know that K_c is a monotonically increasing function of $|h|$, and intend to optimize the power-law approximation exactly at K_c. Hence we have to vary a such that

$$\max_a F(y)|_{\alpha} = 0. \tag{F3}$$

Projection of the maximum on the $|h|$ axis then yields the corresponding threshold values $|h|_c(\alpha)$ at which the approximation for the given α is optimal (Fig. 18). Inversion of this relation allows us to plot the corresponding values of the function $\alpha(|h|)$ (Fig. 8).

Last, let us estimate the asymptotic scaling of $\alpha(|h|)$. If we apply the asymptotic scaling relation for K_c derived in Appendix D, we can approximate

$$\frac{h^2}{2\ln|h|} = a(|h|)|h|^{\alpha(|h|)}. \tag{F4}$$

Taking logarithms, this yields

$$2\ln|h| - \ln 2 - \ln\ln|h| = \ln a(|h|) + \alpha(|h|)\ln|h|. \tag{F5}$$

We now consider variations of α only, i.e., we fix a with respect to $|h|$. Taking the derivative with respect to $|h|$ on both sides of the equation and solving for α then yields

$$\alpha(|h|) \approx 2 - \frac{1}{\ln|h|}. \tag{F6}$$

Inserting this result into Eq. (F5), we finally obtain the estimate

$$a(|h|) \approx \frac{e}{2\ln|h|} \tag{F7}$$

for the proportionality constant a.

[1] S. A. Kauffman, J. Theor. Biol. **22**, 437 (1969).
[2] S. A. Kauffman, *The Origins of Order: Self-Organization and Selection in Evolution* (Oxford University Press, New York, 1993).
[3] B. Derrida and Y. Pomeau, Europhys. Lett. **1**, 45 (1986).
[4] R. V. Solé and B. Luque, Phys. Lett. A **196**, 331 (1995).
[5] B. Luque and R. V. Solé, Phys. Rev. E **55**, 257 (1997).
[6] B. Drossel, in *Reviews of Nonlinear Dynamics and Complexity*, edited by H.-G. Schuster (Wiley VCH, Berlin, 2008).
[7] B. Samuelsson and C. Troein, Phys. Rev. Lett. **90**, 098701 (2003).
[8] R. Albert and A. L. Barabási, Phys. Rev. Lett. **84**, 5660 (2000).
[9] V. Kaufman, T. Mihaljev, and B. Drossel, Phys. Rev. E **72**, 046124 (2005).
[10] T. Mihaljev and B. Drossel, Phys. Rev. E **74**, 046101 (2006).
[11] T. Rohlf, N. Gulbahce, and C. Teuscher, Phys. Rev. Lett. **99**, 248701 (2007).
[12] M. Leone, A. Pagnani, G. Parisi, and O. Zagordi, J. Stat. Mech.: Theory Exp. (2006) P12012.
[13] R. Albert and H. G. Othmer, J. Theor. Biol. **223**, 1 (2003).
[14] S. Braunewell and S. Bornholdt, J. Theor. Biol. **245**, 638 (2007).
[15] P. Ramö, J. Kesseli, and O. Yli-Harja, J. Theor. Biol. **242**, 164 (2006).
[16] T. Rohlf and S. Bornholdt, J. Stat. Mech.: Theory Exp. (2005), L12001.
[17] E. R. Jackson *et al.*, J. Theor. Biol. **119**, 379 (1986).
[18] S. Bornholdt and T. Rohlf, Phys. Rev. Lett. **84**, 6114 (2000).
[19] S. Bornholdt and T. Röhl, Phys. Rev. E **67**, 066118 (2003).
[20] M. Liu and K. E. Bassler, Phys. Rev. E **74**, 041910 (2006).
[21] A. A. Moreira and L. A. N. Amaral, Phys. Rev. Lett. **94**, 218702 (2005).
[22] K. E. Kürten, Phys. Lett. A **129**, 157 (1988).
[23] K. E. Kürten, J. Phys. A **21**, L615 (1988).
[24] T. Rohlf and S. Bornholdt, Physica A **310**, 245 (2002).
[25] I. Nakamura, Eur. Phys. J. B **40**, 217 (2004).
[26] M. Aldana and H. Larralde, Phys. Rev. E **70**, 066130 (2004).
[27] M. Aldana, Physica D **185**, 45 (2003).
[28] F. Greil and B. Drossel, Eur. Phys. J. B **57**, 109 (2007).
[29] S. Patarnello and P. Carnevali, in *Neural Computing Architectures—The Design of Brain-like Machines*, edited by I. Aleksander (MIT Press, Cambridge, MA, 1989).
[30] N. Bertschinger and T. Natschläger, Neural Comput. **16**, 1413 (2004).
[31] A. F. Bompfünewerer *et al.*, Theory Biosci. **123**, 301 (2005).
[32] E. V. Makeyev and T. Maniatis, Science **319**, 1789 (2008).
[33] P. Amaral, M. E. Dinger, T. R. Mercer, and J. S. Mattick, Science **319**, 1787 (2008).
[34] A. Wagner, Proc. Natl. Acad. Sci. U.S.A. **91**, 4387 (1994).
[35] S. Bornholdt and K. Sneppen, Proc. R. Soc. London, Ser. B **267**, 2281 (2000).
[36] S. Ciliberti, O. C. Martin, and A. Wagner, Proc. Natl. Acad. Sci. U.S.A. **104**, 13591 (2007).
[37] We restrict ourselves to negative (or zero) thresholds, to ensure that the "default state" of a network site i, i.e., when its inputs sum to zero, is to be "inactive" ($\sigma_i=-1$), which naturally excludes positive thresholds.
[38] Other authors define $\mathrm{sgn}(0)=+1$, however, for symmetry reasons update dynamics is not affected by either choice. If we interpret the state $\sigma_i=-1$ as "inactive" and, correspondingly, +1 as "active," our choice appears to be more natural: the default state of a network site is to be inactive, unless it receives activating inputs from other sites.
[39] In this context we would like to note that the reasoning provided in Ref. [24] for the derivation of Eq. (9) [the corresponding equation is Eq. (15) in Ref. [24]] is incorrect. In particular, Ref. [24] does not state that the average in $\langle p_s \rangle$ is defined for uniform link selection rather than for uniform node selection,

which can lead to wrong conclusions. These issues are discussed in more detail in Appendix B.

[40] To obtain accurate results, one has to consider networks sizes $N \gg \bar{K}$, and adjust the upper limit of the sum in Eq. (9) accordingly. Since a small step size $\Delta\bar{K}$ has to be applied iteratedly to identify K_c, this becomes computationally very costly.

[41] B. Derrida, in *Fundamental Problems in Statistical Mechanics VII*, edited by H. van Beijeren (North-Holland, Amsterdam, 1990).

[42] T. Rohlf, Europhys. Lett. **84**, 10004 (2008).

[43] P. Fronczak and A. Fronczak, J. Phys. A **41**, 224009 (2008).

[44] A. Szejka, T. Mihaljev, and B. Drossel, New J. Phys. **10**, 063009 (2008).

[45] J. Kesseli, P. Ramö, and O. Yli-Harja, Phys. Rev. E **74**, 046104 (2006).

[46] W. Reik, W. Dean, and J. Walter, Science **293**, 1089 (2001).